

IDENTIFYING SWING MODE BIFURCATIONS AND ASSOCIATED LIMITS ON AVAILABLE TRANSFER CAPABILITY

Christopher L. DeMarco
Department of Electrical and Computer Engineering
University of Wisconsin-Madison
1415 Engineering Drive; Madison, WI USA 53706

Abstract

Analytic techniques for predicting onset of voltage collapse in power systems often rely upon identification of a saddle node bifurcation. While many authors acknowledge that the separation between voltage phenomena and phase angle phenomena is far from absolute, most recent works have viewed voltage variation as the more significant problem. The goal of the work presented here is to shift focus back to loss of stability mechanisms associated with phase angle behavior and electromechanical swing modes. We will exploit structural features in the network to identify a typical form for the eigenvector associated with a bifurcating "swing mode" that reduces in frequency and ultimately loses stability. In a simple case study, we demonstrate that the participation of angles in such a mode is greater than that of voltages.

I. Introduction and Motivation

Over the past decade a considerable body of research and computational tools has been developed for identifying threats to power system security that arise from voltage collapse. Many of these methods compute parameter limits at which the system operating point undergoes a bifurcation. The majority of techniques have focused on loss of stability associated with an isolated real eigenvalue of an appropriate linearization¹ passing from the left half plane to the right half plane (a saddle node bifurcation). Several authors have also noted that the nature of power system dynamics is such that a clean separation of phenomena primarily involving voltage magnitudes from phenomena involving phase angles is not always possible. However, primary focus has been on instabilities that show the greatest participation in voltage variables. If one assumes the

¹Identifying precisely *which* Jacobian is relevant, and the relation of these Jacobians to blocks of a power flow Jacobian or linearized state space model has been a key point of discussion in the literature. See, for example, [1], [2].

typical model of differential equations with algebraic constraints, this may be interpreted as focusing on loss of stability for a generalized eigenvalue that has an associated right eigenvector whose most significant components² are in those locations corresponding to bus voltages. Less work has been conducted in the last decade to look at possible bifurcations of modes that are primarily electromechanical, though an interesting exception is found in the work [4]. To distinguish the work to be presented here from that of [4], note that the "flutter instability" studied in that work relates to a bifurcation in which a complex conjugate pair of eigenvalues migrates to the right half plane. The work to be presented here will focus on a mechanism in which a complex pair first coalesces on the negative real axis, splits, and then a single real eigenvalue crosses into the right half plane.

II. Structural Features of Linearized Models for Electromechanical Dynamics

Strong structural features that arise in linearized dynamics of power systems relate to the fact that power system models consist roughly of second order oscillators coupled through the non-linear power flow of the network. When linearized, the important effects of the coupling show up in a matrix structure closely related to that of a nodal admittance matrix. A number of authors (for example, [2], [5]) have summarized these features in various ways. With this "admittance-like" matrix describing the coupling, one manner in which a zero eigenvalue can be introduced is for a cutset of branches to have zero coefficients (in the graph associated with the admittance matrix). This simple idea is the foundation of the instability mechanism to be studied in this paper. For

²The question of identifying "most significant" components of an eigenvector when the states have different physical units and normalization schemes can sometimes be difficult [3]. However, for the simple dynamic model to be employed here, a naive interpretation of "significance" based on relative magnitude of components of the right eigenvector is judged adequate.

completeness, and development of notation, we shall review some results on model structure [7].

Consider an augmented power system network of n buses, with those numbered 1 through m representing the internal voltage of synchronous generators, and the remainder representing generator terminals and loads. The network is augmented in the sense that generator internal bus voltages are explicitly represented, with an appropriate series reactance (transient reactance of the synchronous machine) connecting the internal bus to terminal bus; a simple classical representation of constant internal bus voltage magnitude is assumed. The equilibrium system frequency is equal a known value of ω_0 .

It will prove convenient to impose assumptions that yield a symmetric power flow Jacobian (provided reactive equations are normalized by voltage magnitude), as is done in stability studies that require existence of a path independent system energy function [8]. We initially neglect rotational damping/governor action, but will re-introduce this effect in our example. With these assumptions, the dynamic equations for the system will possess a modified Hamiltonian form, which yields a simple closed form relationship between real eigenvalues of a reduced dimension, symmetric problem, and eigenvalues of the full dimension, linearized dynamic equations.

To describe this model, let:

- $\mathbf{V} \in \mathbb{R}^n$, $\mathbf{V} :=$ vector of bus voltage magnitudes;
- $\mathbf{\theta} \in \mathbb{R}^n$, $\mathbf{\theta} :=$ vector of bus voltage phase angles relative to an arbitrary synchronous reference frame of frequency ω_0 (no reference angle is deleted);
- $\mathbf{\omega} \in \mathbb{R}^m$, $\mathbf{\omega} :=$ vector of generator frequency deviations, relative to synchronous frequency ω_0 ;
- $\mathbf{M} \in \mathbb{R}^{m \times m}$, $\mathbf{M} :=$ diagonal matrix of normalized generator inertias;
- $\mathbf{P}^I \in \mathbb{R}^n$, $\mathbf{P}^I :=$ vector of net active power injection at each bus; assumed constant;
- $\mathbf{Q}^I: \mathbb{R}^{n-m} \times \mathbb{R}^{n-m}$, $\mathbf{Q}^I(\mathbf{V}) :=$ vector valued function of net reactive power injection at load buses, normalized by voltage magnitude;
- $\mathbf{L}_1 :=$ rows 1 through m of an $n \times n$ identity matrix;

- $\mathbf{L}_2 :=$ rows $m+1$ through n of an $n \times n$ identity matrix;
- $\mathbf{P}^N(\mathbf{V}) :=$ vector-valued function of active power absorbed by network at each bus
- $\mathbf{Q}^N(\mathbf{V}) :=$ vector-valued function of reactive power absorbed by network at load buses, normalized by voltage magnitude

Note that because we have chosen to maintain all voltage angles as states, the model that results is not a minimal realization. The linearization will have a fixed eigenvalue at zero associated with uniform translational motion of angles (see [8] for discussion of minimum versus non-minimum state models).

With the above notation, the resulting nonlinear model for the rotational dynamics of machines coupled through power exchange in the network may be written as follows:

$$\begin{aligned} \dot{\mathbf{M}} &= \mathbf{L}_1(\mathbf{P}^I - \mathbf{P}^N(\mathbf{V})) \\ \dot{\mathbf{L}}_1 &= \\ \mathbf{0} &= \mathbf{L}_2(\mathbf{P}^I - \mathbf{P}^N(\mathbf{V})) \\ \mathbf{0} &= (\mathbf{Q}^I(\mathbf{V}) - \mathbf{Q}^N(\mathbf{V})) \end{aligned}$$

A linearization of these equation about an equilibrium $(\mathbf{0}, \mathbf{\theta}^e, \mathbf{V}^e)$ is then given in the "singular system" form as

$$\tilde{\mathbf{E}} \dot{\mathbf{x}} = \tilde{\mathbf{R}} \mathbf{x}$$

with

$$\begin{aligned} \tilde{\mathbf{E}} &= \begin{bmatrix} \mathbf{M}_{m \times m} & \mathbf{0} & \mathbf{0} \\ \mathbf{0} & \mathbf{I}_{m \times m} & \mathbf{0} \\ \mathbf{0} & \mathbf{0} & \mathbf{0}_{2(n-m) \times 2(n-m)} \end{bmatrix} \\ \tilde{\mathbf{R}} &= \begin{bmatrix} \mathbf{0} & -\mathbf{I}_{m \times m} & \mathbf{0} \\ \mathbf{I}_{m \times m} & \mathbf{0} & \mathbf{0} \\ \mathbf{0} & \mathbf{0} & \mathbf{I}_{2(n-m) \times 2(n-m)} \end{bmatrix} \quad \xi \\ \mathbf{S} &= \begin{bmatrix} \mathbf{I}_{m \times m} & \mathbf{0} & \mathbf{0} \\ \mathbf{0} & \mathbf{J}_{11} & \mathbf{J}_{12} \\ \mathbf{0} & \mathbf{J}_{21} & \mathbf{J}_{22} \end{bmatrix} \\ \mathbf{J} &: \mathbb{R}^n \times \mathbb{R}^{n-m} \times \mathbb{R}^{(2n-m) \times (2n-m)}, \mathbf{J} = \\ & \begin{bmatrix} \frac{\mathbf{P}^N}{\mathbf{V}_L} & \frac{\mathbf{P}^N}{\mathbf{V}_L} \\ \frac{\mathbf{Q}^N}{\mathbf{V}_L} & \frac{\{\mathbf{Q}^N - \mathbf{Q}^I\}}{\mathbf{V}_L} \end{bmatrix} \end{aligned}$$

Next, let us consider a relationship between the generalized eigenvalue problem of interest, and a reduced dimension, symmetric generalized eigenvalue problem in which the power flow Jacobian enters in a direct way. In particular, consider the reduced generalized eigenvalue problem defined by (\mathbf{E}, \mathbf{J}) , where

$$\mathbf{E} = \begin{bmatrix} \mathbf{M} & \mathbf{0} \\ \mathbf{0} & \mathbf{0}_{2(n-m) \times 2(n-m)} \end{bmatrix}$$

Proposition

Assume (\mathbf{E}, \mathbf{R}) has a finite generalized eigenvalue λ , with right eigenvector $\mathbf{v} \in \mathbb{R}^{2n-m}$, $\mathbf{v} = [\mathbf{v}_1^T, \mathbf{v}_2^T]^T$; i.e. $\mathbf{E}\mathbf{v} = \mathbf{R}\mathbf{v}$. Then there exists a $\mathbf{w} \in \mathbb{C}^{2n}$ such that (λ, \mathbf{w}) satisfies $\tilde{\mathbf{E}}\mathbf{w} = \tilde{\mathbf{R}}\mathbf{w}$, with $\lambda = j\sqrt{\cdot}$.

Proof

Minor variation on that of Proposition 2 in [7].

Observation

The result of Proposition 2 indicates that if we wish to examine the behavior of eigenvalues with respect to operating point (e.g., bifurcation behavior) in the non-symmetric generalized eigenvalue problem of $(\tilde{\mathbf{E}}, \tilde{\mathbf{R}})$, we may do so in the context of the reduced dimension, symmetric generalized eigenvalue problem (\mathbf{E}, \mathbf{J}) .

Consequences

i) Suppose that (\mathbf{E}, \mathbf{J}) at an operating point of interest has all its finite generalized eigenvalues non-negative. All finite generalized eigenvalues of $(\tilde{\mathbf{E}}, \tilde{\mathbf{R}})$ must appear on the j axis. It is a straightforward exercise to show that if linear rotational damping is added in every generator component (which provides a very rough approximation to governor action), all finite eigenvalues save one are shifted to the left, and one finite eigenvalue remains fixed at zero.

ii) Consider now a possible route to loss of stability, starting from a stable operating point with the properties assumed in (i). One could hypothesize a gradual change in operating point that would bring one of the positive, finite eigenvalues of (\mathbf{E}, \mathbf{J}) to the origin. In the full problem, $(\tilde{\mathbf{E}}, \tilde{\mathbf{R}})$, with small damping, one would have a complex pair of eigenvalues moving parallel to the j axis. Very near to the parameter values for which the eigenvalue of (\mathbf{E}, \mathbf{J}) reaches zero, a critical complex pair of $(\tilde{\mathbf{E}}, \tilde{\mathbf{R}})$ coalesces to a double real eigenvalue on the negative

real axis. Precisely *at* the parameter values for which (\mathbf{E}, \mathbf{J}) has a new zero eigenvalue, $(\tilde{\mathbf{E}}, \tilde{\mathbf{R}})$ must also have an additional zero eigenvalue. As we will illustrate in the example to follow, this new zero eigenvalue in $(\tilde{\mathbf{E}}, \tilde{\mathbf{R}})$ comes about as the pair which coalesced on the real axis splits, sending one of the pair through the origin. Also note that if parameters move further, beyond the values which yield this singularity, the equilibrium at which the linearization was being evaluated typically ceases to exist.

iii) Finally, note that the motion of this eigenpair will not be differentiable with respect to the parameters at the critical parameter value for which the complex pair coalesce to a repeated real root. Indeed, as we approach this point, the derivative of the eigenvalue motion with respect to parameters approaches infinity. This, of course, is typical in bifurcation problems, but its practical impact is important. The example to follow will illustrate.

The key insight into network structure that is used in our algorithm is quite simple, and may be summarized as follows. The critical complex pair of eigenvalues represents a low frequency swing mode. As the paper title indicates, our interest is in low frequency modes associated with large transfers of active power through a transmission corridor. Under these circumstances, the low frequency swing mode will be an inter-area mode, describing generators on one side of the transmission corridor "swinging" coherently relative to generators on the other side of the transmission corridor, which are also assumed to swing as a coherent group. In this scenario, the associated generalized right eigenvector of the full dynamic model, $(\tilde{\mathbf{E}}, \tilde{\mathbf{R}})$, has a special form. The components of the eigenvector associated with generator angles will show values 180 degrees out of phase on either side of the cutset formed by the transmission corridor. We assume that this structure of eigenvector persists to the point of bifurcation, were the complex pair to split, and one of the resulting real eigenvalues is zero. In other words, we will formulate a system of equations to solve that forces the system $(\tilde{\mathbf{E}}, \tilde{\mathbf{R}})$ to have an "extra" zero eigenvalue, with the generator angle components of the associated eigenvector having the special form described here.

III. Computational Formulation and Example

To formulate our problem precisely, we need additional piece of notation; to this end, let

$$\mathbf{P}^M \in \mathbb{R}^m$$

be the active power injections at generator buses. These are a subset of the $\mathbf{P}^I \in \mathbb{R}^n$ vector introduced earlier, and will be the only components of \mathbf{P}^I to be viewed as unknowns. For compactness, it is also useful to define the overall power mismatch function

$$\begin{aligned} \mathbf{f}(\tilde{\boldsymbol{\theta}}, \mathbf{V}, \mathbf{P}^M) \\ := [(\mathbf{P}^I - \mathbf{P}^N(\tilde{\boldsymbol{\theta}}, \mathbf{V}))^T, (\mathbf{Q}^I(\mathbf{V}) - \mathbf{Q}^N(\tilde{\boldsymbol{\theta}}, \mathbf{V}))^T]^T \end{aligned}$$

Finally, we shall assume that we are seeking a right eigenvector of \mathbf{J} , associated with a zero eigenvalue, that has generator angle components with values given by $[\mathbf{1}^T, -\mathbf{1}^T]^T$, with α a positive real scalar. This enforces the assumption of an inter-area swing mode, as described above. Note also that once we restrict our attention to solving for a zero eigenvalue, it does not matter whether we consider the generalized eigenvalue problem of (\mathbf{E}, \mathbf{J}) , or simply enforce singularity in \mathbf{J} itself.

Given the dimensions of our partitioning scheme, specifying the generator angle components of the eigenvector leaves $2n-2m$ components of the eigenvector as unknowns. Let us denote these remaining eigenvector components as \mathbf{w} . Then our problem may be succinctly stated as follows. Given load demand components of \mathbf{P}^I , \mathbf{Q}^I , solve for $(\tilde{\boldsymbol{\theta}}, \mathbf{V}, \mathbf{P}^M, \mathbf{w})$ satisfying:

$$\mathbf{0} = \mathbf{f}(\tilde{\boldsymbol{\theta}}, \mathbf{V}, \mathbf{P}^M)$$

$$\mathbf{0} = \mathbf{J}(\tilde{\boldsymbol{\theta}}, \mathbf{V})[\mathbf{1}^T, -\mathbf{1}^T, \mathbf{w}^T]^T$$

While this formulation is technically correct, the assumption of a lossless network implies linear dependence between equations. In particular, the sum of all active power equations components must be identically zero for any operating point. Given this dependence, we may discard one row of $\mathbf{f}(\tilde{\boldsymbol{\theta}}, \mathbf{V}, \mathbf{P}^M)$, and one row of $\mathbf{J}(\tilde{\boldsymbol{\theta}}, \mathbf{V})$. Moreover, the unknowns of the generation dispatch vector, \mathbf{P}^M , appear linearly in the associated components of the $\mathbf{f}(\tilde{\boldsymbol{\theta}}, \mathbf{V}, \mathbf{P}^M)=0$ constraint, and may be computed as "outputs" after the desired $(\tilde{\boldsymbol{\theta}}, \mathbf{V})$ is identified. Hence, all m rows of the $\mathbf{f}(\tilde{\boldsymbol{\theta}}, \mathbf{V}, \mathbf{P}^M)=0$ corresponding internal generator buses may be deleted. Denote the resulting reduced dimension quantities respectively as $\tilde{\mathbf{f}}$ and $\tilde{\mathbf{J}}$. Finally,

while it was convenient in Section II to develop the dynamic equations keeping all phase angles as variables, this is not convenient when formulating a Newton-Raphson algorithm to solve the equation set above. Rather, we follow the standard practice of selecting generator angle #1 as reference, and delete that angle from variables for which we solve; denote the reduced vector as $\tilde{\boldsymbol{\theta}}$. In the reduced Jacobian, $\tilde{\mathbf{J}}$, the eigenvector associated with the remaining zero eigenvalue can now take the form $[\mathbf{0}, \mathbf{1}^T, \mathbf{w}^T]^T$, rather than its original form of $[\mathbf{1}^T, -\mathbf{1}^T, \mathbf{w}^T]^T$. In this process, we eliminate the scalar α as an unknown. With these modifications, we are left with the constraint equations:

$$\mathbf{0} = \tilde{\mathbf{f}}(\tilde{\boldsymbol{\theta}}, \mathbf{V}) \quad (1a)$$

$$\mathbf{0} = \tilde{\mathbf{J}}(\tilde{\boldsymbol{\theta}}, \mathbf{V})[\mathbf{0}, \mathbf{1}^T, \mathbf{w}^T]^T \quad (1b)$$

We now have a dimensionally consistent set of equations in the unknowns $(\tilde{\boldsymbol{\theta}}, \mathbf{V}, \mathbf{w})$. While we will not attempt to offer a proof of that the associated Jacobian is generically nonsingular, numerical experience to date suggests that a Newton-Raphson iteration for (1) is typically well-conditioned.

Studies to date have employed a heuristic mix of human judgment in selecting an initial operating point, coupled with the Newton-Raphson algorithm to solve (1). An operating point is selected that produces a heavily loaded corridor in the system. A cutset is selected whose branches include all lines the transmission corridor, and which separates two subsets of generators, one on either side of the cutset. This identifies which components of generator angles are assigned values 0 or 1 in the eigenvector (0's for those generators on the same side of the cutset as the reference bus, 1's for those generators on the opposite side). An inverse power method is used to identify the smallest magnitude eigenvalue of $\tilde{\mathbf{J}}(\tilde{\boldsymbol{\theta}}, \mathbf{V})$, and its associated eigenvector. Those components of the eigenvector not associated with generator phase angles determine the initial guess for \mathbf{w} .

To illustrate this process, consider a network that is a slightly modified version of the IEEE 14 bus system, illustrated below in Figure 1 (the synchronous condensators of that test case are here replaced with standard generators). Table 1 identifies the initial operating point selected, as well as the operating point obtained as the solution of (1).

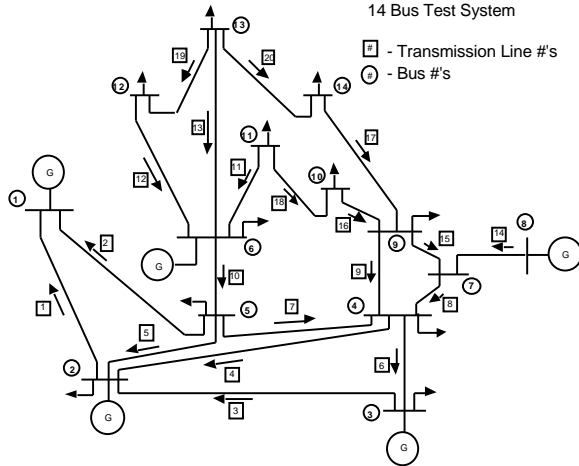


Figure 1: 14 Bus Test System

Table 1: Original & Critical Operating Pnts.

Bus #	Original Op. Point		Critical Op. Point	
	Voltage	Phase(degrees)	Voltage	Phase(degrees)
1	1.0600	0	1.0600	0
2	1.0450	-4.7545	1.0450	-3.3284
3	1.0800	-2.8056	1.0800	-6.4522
4	0.9196	-25.1819	0.8351	-28.9282
5	0.9476	-23.6900	0.8733	-26.8531
6	1.0200	-70.0082	1.0200	-84.2610
7	0.9514	-62.1503	0.8663	-79.5870
8	1.0400	-58.2712	1.0400	-79.4164
9	0.9407	-76.0226	0.8562	-94.5890
10	0.9426	-83.9820	0.8702	-103.0148
11	0.9852	-87.8051	0.9412	-105.1052
12	0.9478	-90.6433	0.9385	-105.5251
13	1.0056	-82.1261	0.9884	-97.3412
14	0.9960	-89.9647	0.9410	-108.4568

To provide further insight into the dynamic interpretation of these results, we performed the following computations. A sequence of operating points were computed, corresponding to a linear interpolation between the generation dispatch for the two operating points identified in Table 1 (loads are unchanged between the two operating points). In a linearized swing dynamic model of the form described in section II, with small rotational damping added at each machine, the finite eigenvalues were calculated for this sequence of operating points. The resulting locus of finite eigenvalues of the dynamic model is illustrated in Figure 2, with an expanded view of the critical eigenvalues in Figure 3. Note that, as predicted, the critical operating point is associated with a complex conjugate pair of eigenvalues coalescing on the negative real axis, splitting, with one of the resulting real eigenvalues moving to the origin. As a final piece of information, the generalized eigenvectors associated with selected

eigenvalues of interest are shown in Table 2, with a one shown for the original operating point, and several for the critical operating point.

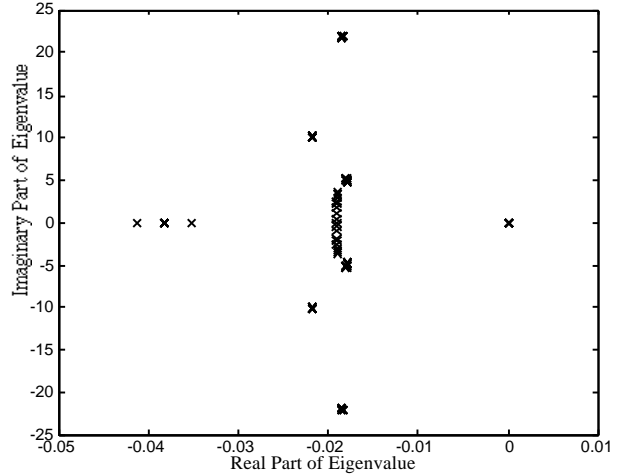


Figure 2: Scatter Plot of Eigenvalues

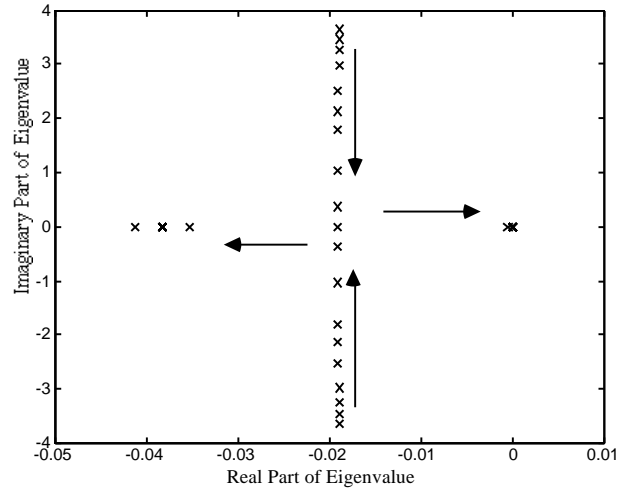


Figure 3: Expanded View Critical Eigenvalues

IV. Conclusions

By imposing a constraint on the nature of the associated eigenvector, we have identified a loss of stability mechanism via a saddle node bifurcation that would appear distinct from those previously examined in voltage collapse studies. The algorithm for computing the critical point is shown to be quite simple to implement. This mechanism of stability loss could be practically important in the evolving competitive utility environment, in which large active power transfers across transmission corridors will be increasingly common and variable. Should this prove true, we believe that this type of bifurcation will warrant further study, as it will impose an important constraint on available transmission capability.

V. Acknowledgment

Partial support of this work has been provided by National Science Foundation and industrial sponsors through the PSerc Industry/University Cooperative Research Center for Power Systems, and by the Western Area Power Administration. This support is gratefully acknowledged.

VI. References

- [1] Y. Mansour, ed. "Suggested Techniques for Voltage Stability Analysis," IEEE Power Engineering Society, publication #93TH0620-5PWR.
- [2] P.W. Sauer and M.A. Pai, "Power System Steady State Stability and the Load-Flow Jacobian," *IEEE Trans. on Power Systems*, vol. 5, no. 4, pp. 1374-1383, Nov. 1990.
- [3] G.C. Verghese, I.J. Pérez-Arriaga, F.C. Schweppe, and K.W-K. Tsai, "Slective Modal Analysis in Power Systems," Electric power Research Institute Report 1764-8, January 1983.
- [4] H.G. Kwatny and X-M. Yu, "Energy ANalysis of Load-Induced Flutter Instability in Classical Models of Electric Power Systems," *IEEE Trans. on Circuits and Systems*, vol. 36, no. 12, pp. 1544-1557, Dec. 1989.
- [5] *Time-Scale Modeling of Dynamic Networks with Applications to Power Systems*, J. H. Chow, ed., Springer-Verlag, Berlin, 1982.
- [6] J. H. Chow, "New Algorithms for Slow Coherency Aggregation of Large Power Systems," from **Systems and Control Theory for Power Systems**, J. H. Chow, P. V. Kokotovic, R. J. Thomas, ed., Springer-Verlag, New York, 1995.
- [7] C. L. DeMarco and J. J. Wasner , "A generalized eigenvalue perturbation approach to coherency," pp. 605-610, *Proc. IEEE Conference on Control Applications*, Albany, NY, Sept. 28-29 1995.
- [8] M. A. Pai, **Energy Function Analysis for Power System Stability**, Kluwer Academic Publishers, Boston, 1989.
- [9] **MATLAB User's Guide**, The MathWorks, Inc., Natick, MA, 1993.

Table 2: Selected Generalized (Right) Eigenvectors of the Full Dynamic Model

State deviation described by eigenvector component	Original Op. Pnt: Evector for lambda = -0.0189 + 3.6342i	Critical Op. Pnt: Evector for lambda = -0.3957	Critical Op. Pnt: Evector for lambda = -0.2294	Critical Op. Pnt: Evector for lambda = 0.0000 (original)	Critical Op. Pnt: Evector for lambda = 0.0000 (newly created)
Freq@Bus 1	-0.4033-0.0048i	-0.0181+0.0000i	-0.0000+0.0000i	0.0000-0.0000i	-0.0000-0.0000i
Freq@Bus 2	-0.3917-0.0047i	-0.0181+0.0000i	-0.0000+0.0000i	0.0000+0.0000i	-0.0000-0.0000i
Freq@Bus 3	-0.4287-0.0051i	-0.0181-0.0000i	-0.0000-0.0000i	0.0000-0.0000i	-0.0000+0.0000i
Freq@Bus 6	0.3068+0.0026i	0.0000-0.0000i	-0.0103-0.0000i	0.0000-0.0000i	0.0000-0.0000i
Freq@Bus 8	0.4964+0.0054i	0.0000+0.0000i	-0.0103+0.0000i	0.0000+0.0000i	0.0000+0.0000i
Angle(radians)@Bus 1	-0.0007+0.1110i	0.4384-0.0000i	0.0000+0.0000i	0.2675-0.0000i	-0.2019+0.0000i
Angle(radians)@Bus 2	-0.0007+0.1078i	0.4384+0.0000i	0.0000-0.0000i	0.2675+0.0000i	-0.2019-0.0000i
Angle(radians)@Bus 3	-0.0008+0.1180i	0.4384+0.0000i	0.0000-0.0000i	0.2675+0.0000i	-0.2019-0.0000i
Angle(radians)@Bus 6	0.0003-0.0844i	-0.0000+0.0000i	0.2924-0.0000i	0.2672-0.0000i	0.2359+0.0000i
Angle(radians)@Bus 8	0.0008-0.1366i	-0.0000+0.0000i	0.2924+0.0000i	0.2672+0.0000i	0.2359-0.0000i
Angle(radians)@Bus 4	-0.0005+0.0625i	0.3689+0.0000i	0.0463+0.0000i	0.2674+0.0000i	-0.1326-0.0000i
Angle(radians)@Bus 5	-0.0005+0.0639i	0.3659+0.0000i	0.0484+0.0000i	0.2674+0.0000i	-0.1295-0.0000i
Angle(radians)@Bus 7	0.0004-0.0868i	-0.0005-0.0000i	0.2928-0.0000i	0.2672-0.0000i	0.2364+0.0000i
Angle(radians)@Bus 9	0.0005-0.1030i	-0.0799-0.0000i	0.3457+0.0000i	0.2671-0.0000i	0.3156+0.0000i
Angle(radians)@Bus 10	0.0005-0.1130i	-0.1091-0.0000i	0.3652-0.0000i	0.2671-0.0000i	0.3448+0.0000i
Angle(radians)@Bus 11	0.0004-0.1060i	-0.0745-0.0000i	0.3421+0.0000i	0.2671-0.0000i	0.3103+0.0000i
Angle(radians)@Bus 12	0.0003-0.0895i	-0.0159+0.0000i	0.3030+0.0000i	0.2672+0.0000i	0.2517-0.0000i
Angle(radians)@Bus 13	0.0003-0.0912i	-0.0218+0.0000i	0.3069-0.0000i	0.2672+0.0000i	0.2576-0.0000i
Angle(radians)@Bus 14	0.0005-0.1136i	-0.1031-0.0000i	0.3612-0.0000i	0.2671-0.0000i	0.3388+0.0000i
Voltage(pu)@Bus 4	0.0003-0.0569i	-0.1401-0.0000i	0.0935-0.0000i	-0.0001-0.0000i	0.1399+0.0000i
Voltage(pu)@Bus 5	0.0003-0.0502i	-0.1251-0.0000i	0.0834-0.0000i	-0.0001-0.0000i	0.1249+0.0000i
Voltage(pu)@Bus 7	0.0003-0.0548i	-0.1492-0.0000i	0.0995-0.0000i	-0.0001-0.0000i	0.1490+0.0000i
Voltage(pu)@Bus 9	0.0003-0.0564i	-0.1549-0.0000i	0.1033-0.0000i	-0.0001-0.0000i	0.1546+0.0000i
Voltage(pu)@Bus 10	0.0003-0.0483i	-0.1341-0.0000i	0.0894-0.0000i	-0.0001-0.0000i	0.1339+0.0000i
Voltage(pu)@Bus 11	0.0002-0.0272i	-0.0793-0.0000i	0.0529-0.0000i	-0.0001-0.0000i	0.0791+0.0000i
Voltage(pu)@Bus 12	0.0000-0.0052i	-0.0159+0.0000i	0.0106-0.0000i	-0.0000-0.0000i	0.0159-0.0000i
Voltage(pu)@Bus 13	0.0001-0.0101i	-0.0302-0.0000i	0.0202-0.0000i	-0.0000-0.0000i	0.0302-0.0000i
Voltage(pu)@Bus 14	0.0002-0.0364i	-0.1021-0.0000i	0.0681-0.0000i	-0.0001-0.0000i	0.1020+0.0000i